AIAA SciTech 2015, Jan 5–9, Kissimmee, Florida

Numerical Investigation of Upstream Fuel Injection through Porous Media for Scramjet Engines via Surrogate-Assisted Evolutionary Algorithms

H. Ogawa*, B. Capra†, and P. Lorrain‡

Abstract

A multi-objective design optimization study has been conducted for upstream fuel injection through porous media applied to the first ramp of a two-dimensional scramjet intake. The optimization has been performed by coupling evolutionary algorithms assisted by surrogate modeling and computational fluid dynamics with respect to three design criteria, that is, the maximization of the absolute mixing quantity, total pressure saving, and fuel penetration. A distinct Pareto optimal front has been obtained, highlighting the counteracting behavior of the total pressure against the mixing efficiency and fuel penetration. The injector location and size have been identified as the key design parameters as a result of a sensitivity analysis, with negligible influence of the porous properties in the configurations and conditions considered in the present study. Flowfield visualization has revealed the underlying physics associated with the effects of these dominant parameters on the shock structure and intensity.

I. Introduction

HYPERSONIC airbreathing propulsion offers the great potential for reliable, reusable and economical systems for access-to-space and high-speed atmospheric cruise for both civilian and strategic purposes. Scramjet (supersonic combustion ramjet) propulsion, in particular, is a promising technology that can enable efficient and flexible transport systems by removing the need to carry oxidizers and other limitations of conventional rocket engines. The last decade has seen remarkable milestones achieved by various flight experiments including The University of Queensland's HyShot II in July 2002,[1,2] the NASA X-43 vehicles in the Hyper-X program in March and November 2004,[3] and the Boeing X-51A WaveRider in May 2010.[4]

The scramjet mechanism depends critically on the sequential process – capture and compression of hypersonic airflow in the inlet, fuel injection into the air, supersonic combustion in the chamber, and expansion of combustion products for thrust through the nozzle. An axisymmetric scramjet configuration has been explored in ground and flight tests in Australia, following the performance demonstrated in shock tunnel testing.[5,6] It features innovative concepts such as fuel injection on the inlet surface and shock-induced combustion by radical-farming.[7,8] Upstream fuel injection in the inlet surface promotes fuel/air mixing, resulting in a decrease in skin friction as well as vehicle length and structural weight.[9]

Fuel injection plays a major role in the flow process, responsible for efficient combustion and hence overall scramjet performance.[9] In particular, inlet fuel injection is characterized by considerably higher crossflow velocity, as compared to conventional methods where fuel injection takes place downstream into slower airflow due to further compression. The interactions between fuel and air including mixing, ignition and combustion occur at an extremely short timescale, rendering the development of efficient and reliable

*Senior Research Fellow, School of Aerospace, Mechanical and Manufacturing Engineering, RMIT University, Melbourne, VIC 3001, Australia

†Lecturer, School of Chemistry, Physics and Mechanical Engineering, Science and Engineering Faculty, Queensland University of Technology, Brisbane, QLD 4001, Australia

‡Research Associate, School of Engineering and Information Technology, UNSW Canberra, ACT 2600, Australia

fuel injection systems of crucial importance. A variety of fuel injection techniques have been contrived and examined in order to improve the mixing performance as below.

Transverse injection through wall orifices is a common method used to supply fuel, penetrating into the supersonic mainstream. Appreciable benefits in mixing enhancement have been observed in experimental and numerical studies, while fuel penetration has been found to depend on inclination of the injection hole and the orifice shape.[10,11] However, it is commonly reported that this injection method entails considerable total pressure loss due to a bow shock as a result of strong jet-airflow interactions.[12] A recent parametric study performed numerically with *multi-port injection* via regular arrays of very fine fuel injectors suggests that appreciable mixing and penetration with minimum total pressure loss may be achieved by carefully tuning the configurations of the multi-porthole arrays.[13] *Tangential injection*, on the other hand, can introduce fuel into the airflow with minimum disturbance into the mainstream,[14] its streamwise momentum yielding further benefits on the engine performance, which is an increasingly important element for thrust potential at higher speeds.[15] Although penetration is significantly limited with this type of injection, an additional benefit of substantial skin-friction drag reduction is yielded by this method in the event of boundary-layer combustion.[9,16] The use of so-called *hypermixers* is a different approach to improve mixing characteristics owing to streamwise vortices which are introduced by alternating wedges or ramp injectors. The benefits of this technique in mixing and combustion enhancement have been demonstrated experimentally and numerically,[17,18] although device implementation inevitably causes structural penalty and performance losses particularly under off-design conditions. Transverse or inclined injection in the vicinity of a *backward-facing step* or a cavity offers advantages in self ignition and flame holding in the recirculation zone downstream of the step, where injected fuel is mixed with relatively slow airflow at high temperature,[19,20] while characterized by similar drawbacks to those of hypermixers.

Fuel supply through porous media (*porous injection*) is a relatively new method enabled by the advancement of material technologies. A notable effect of this technique on combustion enhancement has been observed in a shock-tunnel experiment recently conducted at The University of Queensland.[21] Figure 1 (a) displays the flowfield visualized by schlieren photography. The surface pressure distributions at the centerline plotted in Fig. 1 (b) indicate that a significantly higher combustion level was achieved with porous injection while benign interactions occurred between the fuel jet and crossflow owing to weaker oblique shock waves, as compared to the case with porthole injection. A numerical investigation in corresponding conditions conducted by Capra *et al.* revealed the detailed characteristics of scramjet intake flowfields in the presence of porous injection.[22] Advantages over porthole (transverse) injection were observed in various aspects including fuel/air mixing enhancement, favorable shock structures, and shorter ignition delay. Another experimental study found porous media effective in enhancing the engine performance from both ignition and combustion perspectives, when used to supply pre-mixed oxygen upstream of injection.[23]

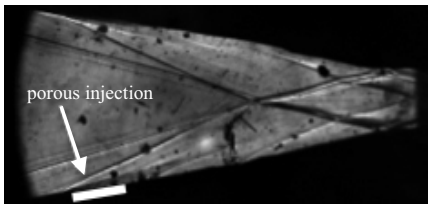

(a) schlieren photo

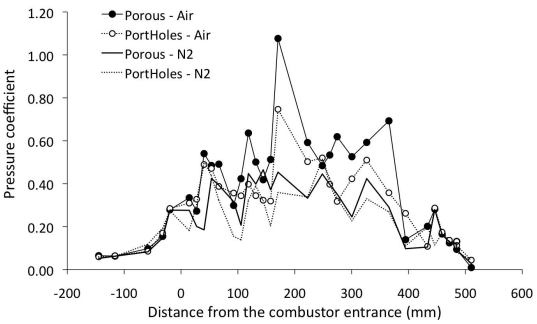

(b) centerline pressure

Figure 1. Flowfield visualization and measurement of scramjet intake with porous injection[21]

Porous-injection flowfields are characterized by the material properties of porous media as well as the geometrical arrangements of the injector. The present research project is undertaken in order to examine the effects of such attributes on the fuel/air mixing characteristics in a coupled numerical approach combining computational fluid dynamics and multi-objective design optimization based on evolutionary algorithms assisted by surrogate modeling. Porous properties and geometric parameters are employed as decision variables for an optimization problem simultaneously aiming at maximum mixing efficiency, minimum total pressure loss, and maximum fuel penetration into crossflow. Flowfields are to be scrutinized for representative individuals selected from the population pool in comparison with those from other injection methods (*e.g.*, transverse injection), and all configurations evaluated in the course of the

optimization process are assessed by means of global sensitivity analysis. Physical insights to be gained from this study will be usefully applicable to the design of high-performance porous injector for scramjet engines.

II. Approaches

A. Configurations and flow conditions

A two-ramp compression intake is considered in the present study in order to replicate the intake section of a nominally two-dimensional scramjet engine that has been previously tested in the T4 shock tunnel of The University of Queensland. It features a combined horizontal length of 179.9 mm (134.9 mm and 45 mm for the first and second ramp) and a turning angle of 12° (9° and 3°, respectively).[24] Fuel injection is achieved through a porous media with the property described below, implemented on the first ramp.

Table 1 shows the freestream conditions assumed in this study. They are based on the results from axisymmetric reacting simulations that have been performed, replicating a known condition of the T4 shock tunnel that produces approximately Mach 6.3 with stagnation enthalpy of 4.5 MJ/kg, equivalent to a Mach 9.67 scramjet flight at an altitude of 30 km.[22] The table also displays the equilibrium chemical composition of the nozzle reservoir air, which is assumed to consist of N, O, O_2, N_2, and NO species.

Table 1. Freestream and fuel plenum conditions

property			freestream	fuel plenum
Mach number			6.44	–
static pressure	p	[kPa]	8.99	–
total pressure	p_0	[kPa]	23428	1413
static temperature	T	[K]	446	–
total temperature	T_0	[K]	4053	700
dynamic pressure	q	[kPa]	69.2	–
Reynolds number	Re	[/m]	7.71×10^6	–
O_2 mass fraction	c_{O_2}		0.2267	–
O mass fraction	c_O		0.0002	–
NO mass fraction	c_{NO}		0.0519	–
H_2 mass fraction	c_{H_2}		0.0000	1.0000

B. Porous injection

Fluid flow through porous media is characterised by pressure drops sustained over the thickness of the media due to two major factors, that is, viscous and inertial effects.[22] The viscous drop is linearly correlated to the average superficial velocity by Darcy's law, while the drop due to inertia is prescribed by Forchheimer's law.[28,29] The material's permeability attributed to these effects is represented in terms of the Darcy and Forchheimer coefficients, respectively. The permeability coefficients considered here are expressed respectively in the tensor form as:

$$\boldsymbol{K_D} = \begin{pmatrix} 1.079\times10^{-13} & 0 & 0 \\ 0 & 7.584\times10^{-13} & 0 \\ 0 & 0 & 7.584\times10^{-13} \end{pmatrix} [\mathrm{m}^2] \quad (1)$$

$$\boldsymbol{K_F} = \begin{pmatrix} 8.065\times10^{-9} & 0 & 0 \\ 0 & 1.229\times10^{-7} & 0 \\ 0 & 0 & 1.229\times10^{-7} \end{pmatrix} [\mathrm{m}] \quad (2)$$

based on the measured properties of the physical samples used in shock tunnel experiment, which were designed and manufactured at DLR Stuttgart,[30] consisting of a Ceramic Matrix Composite structure of carbon-carbon with a porosity of approximately 16%. 28 mm is assumed for the baseline length (l_j) of the

porous injection in this study, based on the injector used in the experiment that was 44.4 mm wide and 28 mm long.[21,22] A streamwise location of 92.33 mm downstream from the intake leading edge is considered as the nominal injector position (x_j) of the baseline configuration.

The fuel (hydrogen) is supplied from a plenum chamber of 12 mm in depth, which allows the fuel flow to establish before entering the porous block, replicating the experimental model. The porous block is tapered at 20° to expand toward the plenum side, whose reservoir conditions are shown in Table 1. The injector arrangement is schematically presented in Fig. 2, superimposed on the computational mesh for the baseline injector.

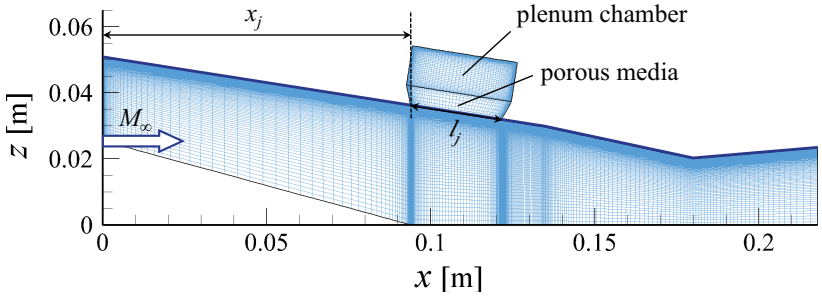

Figure 2. Porous injection setup and computational mesh

C. Computational fluid dynamics

Compressible flowfields in the presence of fuel injection are computed by utilizing a commercial solver CFD++,[31] which has been employed by the Australian hypersonics network for scramjet research due to its demonstrated fidelity in hypersonic aerodynamics.[5,13,22,32,33] An implicit algorithm with second-order spatial accuracy is used to solve the Navier-Stokes equations for viscous flowfields and convergence is accelerated by the multigrid technique. The gas composition is represented by Evans & Schexnayder ' s model,[34] which consists of 25 elementary reactions among 12 species including hydrogen-air combustion and nitrogen reactions, although chemically frozen flow is assumed in the present research. An isothermal wall at a constant temperature of 300 K is assumed for the inlet surface. The boundary layer is taken to be fully turbulent and modeled by the two-equation SST k-ω RANS model. Two-dimensional computational meshes are generated automatically by Glyph scripting on a commercial grid generator Pointwise[35] for the fuel injector configuration represented by the two geometric design variables introduced above.

Porous injection is numerically implemented by applying the following porous source term to the Naveir-Stokes momentum equations:

$$S_i = \left(\sum_{j=1}^{3} \boldsymbol{D_{ij}} \mu u_j + \sum_{j=1}^{3} \frac{1}{2} \boldsymbol{C_{ij}} \rho |u_j| u_j \right) \tag{3}$$

where the tensor matrix coefficients $\boldsymbol{D_{ij}}$ and $\boldsymbol{C_{ij}}$ are user-defined terms for viscous and inertial resistance, respectively.[31] They are reciprocally related to the Darcian-Forchheimer coefficients as $\boldsymbol{D} = \frac{1}{\boldsymbol{K_D}}$ and $\boldsymbol{C} = \frac{2}{\boldsymbol{K_F}}$ with the attributes for the examined porous samples shown in Eqs. (1) and (2), respectively.

D. Evolutionary algorithms

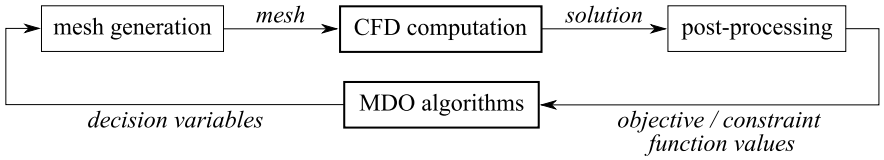

Figure 3. EA-based MDO chain incorporating CFD evaluation

The optimization is performed in an iterative manner in an optimization chain consists of pre-processing, trajectory simulation (evaluation), post-processing, and optimization algorithms, as schematically drawn in Fig. 3. An evolutionary algorithm (EA), in particular, the elitist non-dominated sorting genetic algorithm (NSGA-II),[36,37] is employed for design optimization with multiple objectives.[38,39] Optimization occurs over generations with a certain number of individuals in the population pool. Multiple individuals are evaluated simultaneously by parallel computations (CFD simulations) on multiple CPUs within the resource allowance, which is a notable advantage of population-based algorithms over gradient-based methods.[40] A simulated binary crossover and polynomial mutation are used as recombination operators at a given probability with a specified distribution index.

The optimization process is efficiently assisted by replacing trajectory simulation for the objective and constraint functions with the estimations from surrogate modeling once reasonable correlations between the input (decision variables) and output parameters (objective/constraint functions) are established from an archive of solutions that have been evaluated with CFD simulations (typically after the fifth generation). Surrogate models considered include: response surface models, kriging approximations, and radial basis functions.[39,40] Hybrid operations via pattern search and sequential quadratic programming techniques[41] are performed for selected individuals in conjunction with the EA in order to accelerate the convergence of the Pareto optimal front, once valid surrogate prediction becomes available (simulated annealing can also be employed for non-constrained problems).

Variance-based global sensitivity analysis is performed to investigate the influence of the decision variables on the objective and constraint functions, based on the surrogate models that offer the best prediction accuracy as at the final generation. Evaluation is made for sample data points represented by Sobol quasi-random numbers[43] within the ranges of the decision variables.

E. Performance parameters

Three parameters are considered to quantitatively evaluate the mixing performance of the fuel injectors and employed as the objective functions of the optimization.

- Mixing efficiency
  The mixing ability of the injectors is assessed by the mixing efficiency defined as

$$\eta_m \equiv \frac{1}{\dot{m}_{H_2}} \int \min\Big(c_{H_2}, \frac{c^s_{H_2}}{c^s_{O_2}} c_{O_2}\Big) d\dot{m} \tag{4}$$

  where $\dot{m}$ is the mass flow rate, c is the mass fraction, and the superscript s denotes the stoichiometric values, *i.e.*, c_{H_2} =0.029 and $c_{O_2} = 0.228$, which represent the ratio of fuel (hydrogen) to oxygen needed to completely burn all the available fuel. This parameter serves as an indicator of the fraction of the fuel to be consumed when all mixed gases react. However, it inherently yields higher values for lower fuel/air equivalence ratio Φ by definition.[25] The absolute mixing quantity $\eta_m \times \Phi$ is therefore introduced in lieu of mixing efficiency in order to allow fairer comparison across various Φ values.

- Total pressure recovery
  High total pressure recovery is also a desired feature in fuel mixing, and this objective is aimed at by minimizing the total pressure loss defined as

$$\Delta p_0 \equiv 1 - \frac{\int_x p_0 d\dot{m}}{\int_{x=0} p_0 d\dot{m}} \tag{5}$$

  where p_{01} and p_0 denote the total pressure at the entrance and exit of the intake, respectively. The mass-averaged total pressure on which this measure is based, however, inherently does not satisfy the conservation laws. The following parameter based on the stream-thrust-averaged total pressure[26,27] (denoted as $p_{0\,STA}$), is considered additionally to quantify the total pressure loss, defined as

$$\Delta p_{0\,STA} \equiv 1 - \frac{p_{0\,STA}}{p_{01\,STA}} \tag{6}$$

  where $p_{01\,STA}$ is the stream-thrust-averaged total pressure at the entrance ($x = 0\,\text{mm}$) and $p_{0\,STA}$ is that at the streamwise station of interest.

- Fuel penetration
  The extent of fuel penetration into the core flow is another useful indicator for fuel/air mixing. This criterion is assessed by the distance from the centerline of the injector orifice to the height where the hydrogen mass fraction of the jet plume reduces to 10% of the stoichiometric mass fraction, defined as:

$$h_f \equiv \max\left(z\,|_{c_{H_2}>0.1c^s_{H_2}}\right) \tag{7}$$

  where z denotes the vertical coordinate and $c^s_{H_2}$ the stoichiometric mass fraction of hydrogen.

F. Optimization problem

Two geometric design parameters, *i.e.*, injector position x_j and injector lengthl_j are employed as the decision variables, along with the characteristic quantities of the porous media. In particular, the following four coefficients are selected in relation to the Darcian-Forchheimer coefficients, assuming an anisotropic material attributes: $K_{D_{xx}}$, $K_{D_{yy}}(= K_{D_{zz}})$, $K_{F_{xx}}$, and $K_{F_{yy}}(= K_{F_{zz}})$. Non-dimensionalized quantities (denoted with over lines) are used for all of these decision variables, normalized by the baseline values, that is, $x_j = 0.095\,\mathrm{m}$, $l_j = 0.028\,\mathrm{m}$ and the coefficients in Eqs. (1) and (2) for the porous property. The lower and upper bounds of these parameters are set to allow reasonable variations so that their influence on the objective functions can be examined. The optimization problem statement of this study is thus expressed as[a]:

minimize:	(-) absolute mixing quantity	$-\eta_m \times \Phi$
	total pressure loss	Δp_0
	(-) penetration height	$-h_f$
subject to:	injection position	$0.6 \le \overline{x_j} \le 1.05$
	injection length	$0.5 \le \overline{l_j} \le 1.25$
	Darcian coefficient (x direction)	$0.1 \le \overline{K_{D_{xx}}} \le 10$
	Darcian coefficient (y & z direction)	$0.1 \le \overline{K_{D_{yy}}} \le 10$
	Forchheimer coefficient (x direction)	$0.1 \le \overline{K_{F_{xx}}} \le 10$
	Forchheimer coefficient (y & z direction)	$0.1 \le \overline{K_{F_{yy}}} \le 10$

III. Results

A. Optimization

A CFD-based optimization has been performed by evolving a population comprising 32 individuals over 10 generations via evolutionary algorithms assisted by surrogate modeling. The non-dominated (optimal) solutions are identified among all 288 feasible individuals evaluated in the course in Fig. 4 (a) to explore the design space considered in the present study. Figure 4 (b), on the other hand, shows the Pareto optimal front that resulted from an optimization run with 96 individuals evolved over 50 generations, which has been performed solely depending on the prediction from surrogate models trained using CFD-evaluated solutions, with prediction errors of 0.06%, 0.02% and 0.21% by the kriging approximation.

Figures 5 (b)-(d) display the distributions of the evaluated solutions on projected planes of respective two objective functions, with the color in the dots indicative of the level of the other objective function. Figure 5 (a) displays a distinct Pareto optimal front comprising non-dominated solutions, clearly indicative of a counteracting tendency between the total pressure saving and the absolute mixing quantity. Figure 5 (b), on the other hand, exhibits a remarkably close correlation between the absolute mixing quantity and the fuel penetration height. In consequence a counteracting characteristic is evident between the total pressure saving and fuel penetration in Figure 5 (c).

The properties of the individuals in the final population pool are represented in the form of a parallel coordinate plot in Fig. 6, where the values of the objective functions and those of the decision variables are connected with colored lines for the superior individuals including non-dominated ones, normalized with respect to the range of each parameter. It can be noted that values for the values for the injector position x_j

[a]Negative signs are added to the parameters to be maximized, that is, η_m and h_f, in order to convert maximization problems into minimization ones.

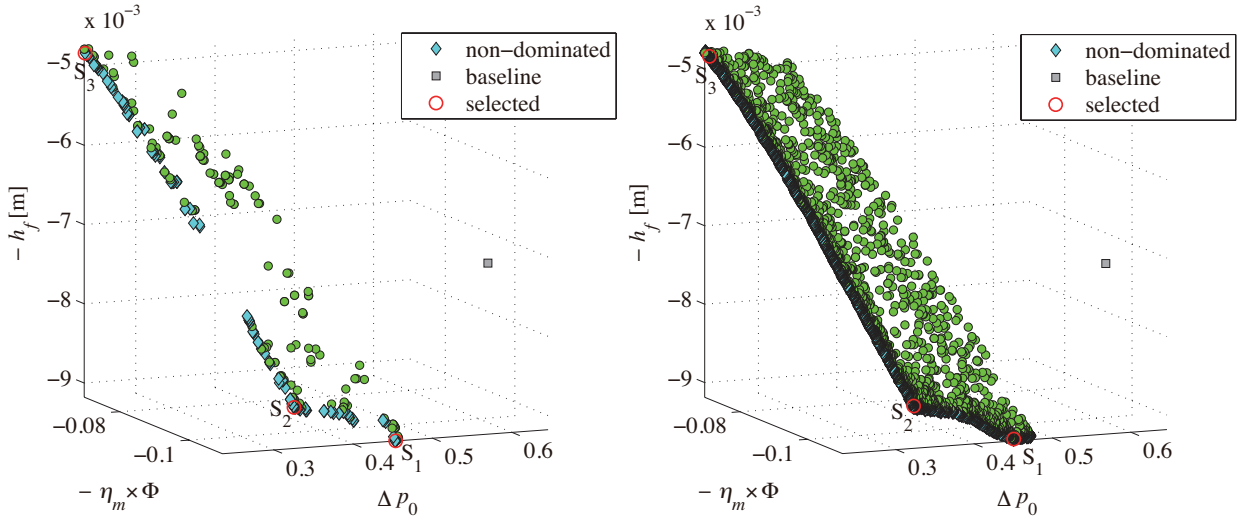

(a) CFD simulation

(b) surrogate prediction

Figure 4. Optimization results from CFD simulation and surrogate prediction

tend to gather near the upper bound (hence preferring downstream positions) for the 'elites' that survived the evolutionary process, while the lines connecting the objective functions cross each other, representing the counteracting behavior.

In order to probe into the results, three representative solutions have carefully been selected from all individuals that have been evaluated by the final generation to facilitate scrutinization and comparison. The trajectories are analyzed in the following section for these selected individuals, referred to as S_1, S_2, and S_3. S_1 offers the maximum absolute mixing quantity, while incurring the maximum total pressure loss. S_3, in contrast, features the minimum total pressure loss (hence maximum saving) while producing the minimum absolute mixing efficiency. S_2 lies on the kink where the Pareto optimal front is inflected, as displayed in Figs. 4 and 5. The values of the objective functions and those of the decision variables (design parameters) are shown in Table 2 for the representative individuals and baseline configuration.

Table 2. Objective function and decision variable values for selected individuals

individual	$\eta_m \times \Phi$	$\Delta p0$	h_f [m]	$\overline{x_j}$	$\overline{l_j}$	$\overline{K_{D_{xx}}}$	$\overline{K_{D_{yy}}}$	$\overline{K_{F_{xx}}}$	$\overline{K_{F_{yy}}}$
S_1	0.110	0.454	0.00918	0.704	1.25	1.86	8.88	9.18	3.41
S_2	0.103	0.353	0.00879	1.045	1.24	1.42	6.72	8.91	2.17
S_3	0.070	0.235	0.00483	1.047	0.512	1.84	7.32	7.32	3.86
baseline	0.092	0.646	0.00739	1	1	1	1	1	1

B. Flowfields

The flowfields associated with the selected individuals and baseline injector are compared in Fig. 8 with respect to the Mach number distributions. An initial oblique shock generated at the leading edge of the intake and a stronger oblique shock due to injection coalesce upstream of the reflection at the symmetry plane. The reflected shock enters the combustor downstream. The comparison between the S_1 and S_2 configurations, which are characterized by virtually the same injector length l_j, indicates that shock reflection takes place upstream for an upstream injector location x_j. The comparison of S_2 with S_3, which do not differ in position but in length, on the other hand, suggests the occurrence of earlier shock reflection with a longer injector due to an augmented oblique shock with an increased amount of fuel injection.

The distributions of the static pressure compared in Fig. 9 commonly show the initial pressure rise across

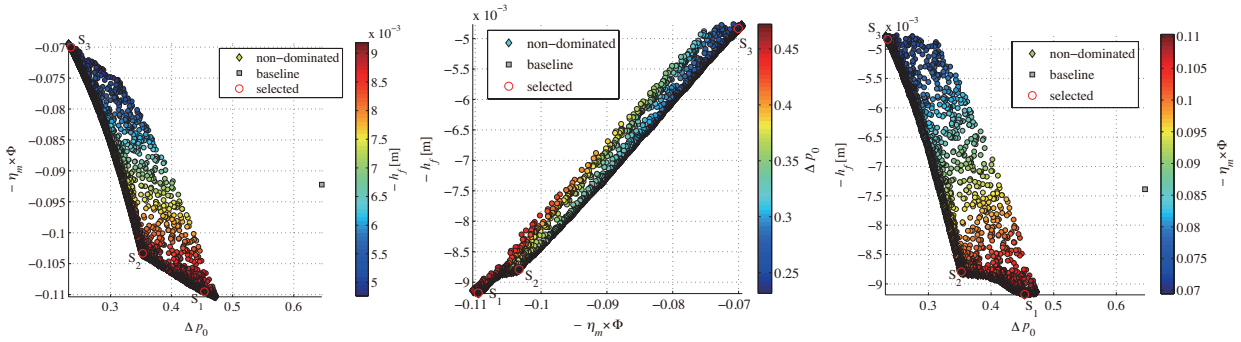

(a) total pressure loss vs absolute mixing quantity

(b) absolute mixing quantity vs fuel penetration

(c) total pressure loss vs fuel penetration

Figure 5. Optimization result in planar views (surrogate-only optimization)

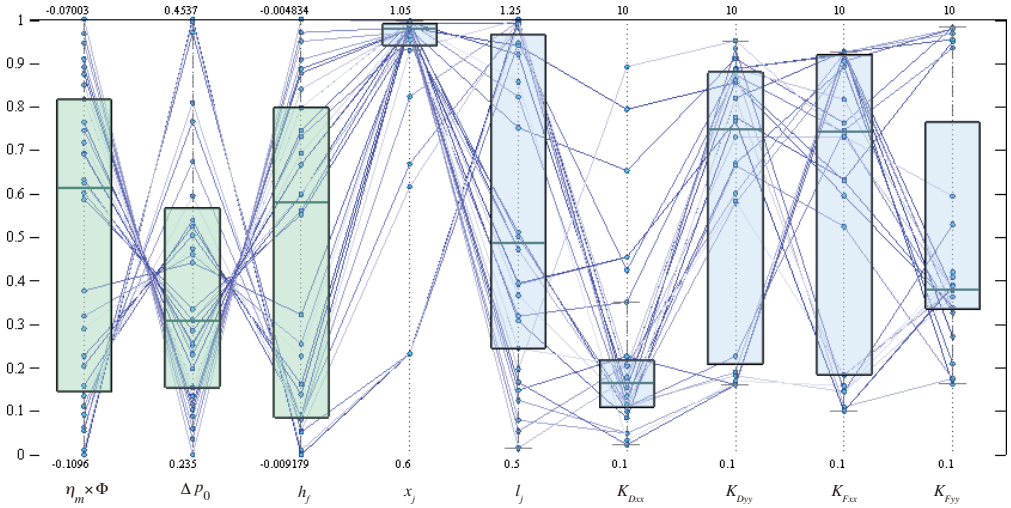

Figure 6. Parallel coordinate plot

the leading-edge shock followed by a larger jump due to the injection shock. The greatest rise is caused by the shock reflection on the symmetry plane. The resultant pressure increase is similar between the baseline and S_1 cases, but augmented when the injector is positioned downstream, as seen in the distribution for the S_2 geometry. In contrast the S_3 configuration with the shortest injector hence least fuel injection is characterized by minimum pressure rise, as also seen in Fig. 12 (a).

The static temperature distributions in Fig. 10 show similar trends to those observed for the static pressure, as found in Fig. 12 (c).

The fuel supplied through longer injectors S_1 and S_2 distribute in a larger extent compared to the baseline configuration in Fig 11. The comparison of S_1 and S_2 suggests that fuel can propagate farther from the surface at the intake exit with an upstream injector position, as seen in Fig. 12 (d). Fuel injection through a short injector (S_3) is characterized by the shortest penetration.

C. Sensitivity analysis

Variance-based global sensitivity analysis is performed to investigate the influence of the decision variables on the objective and functions, based on the surrogate model with the best prediction accuracy as of the final generation. Evaluation is made for 10,000 sample data points represented by Sobol quasi-random numbers within the decision variable ranges.[42,43] The first-order sensitivity indices and total-effect indices are calculated, which represent the main and overall effect of the input parameter (decision variables) on the

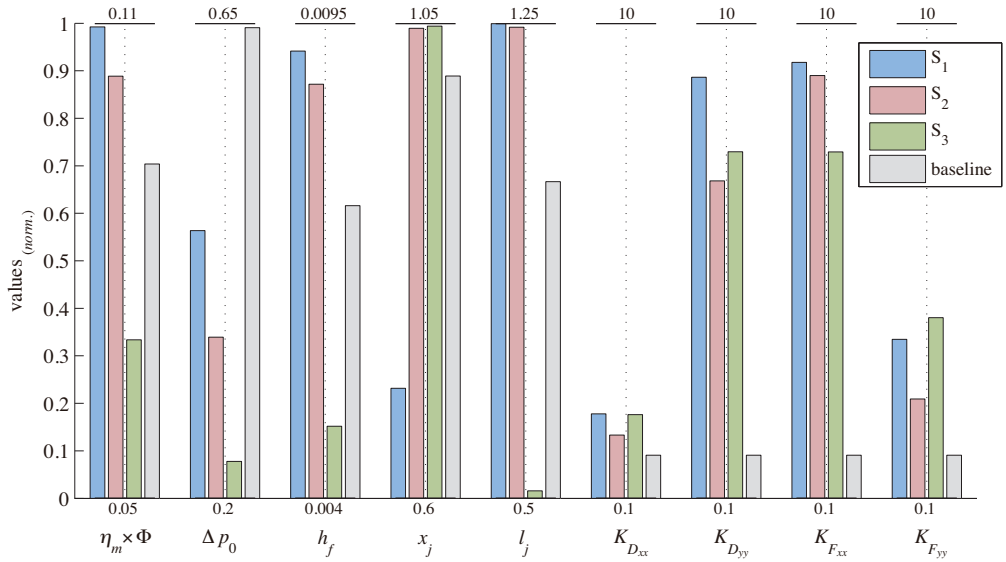

Figure 7. Parameters of selected individuals

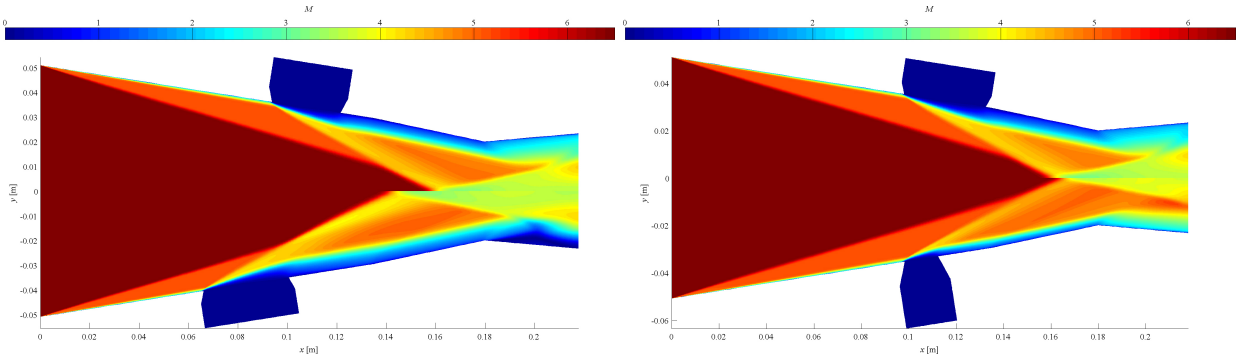

(a) baseline vs S_1

(b) S_2 vs S_3

Figure 8. Comparison of Mach number distributions

output parameters (objective functions), respectively. The difference between the total-effect index S_{T_i} and the first-order index S_i is indicative of the degree of the involvement of the decision variable in interactions with other decision variables.[43] In situations where the sum of both first-order and total-effect indices are near unity, on the other hand, the effects of individual decision variables on the output parameter are linearly additive. The difference between the first-order and total-effect indices indicates a large degree of interactions and involvement of all decision parameters affecting all objective functions.

Figure 13 presents the first-order indices S_i and total-effect indices S_{T_i} for the absolute mixing quantity, total pressure loss, and fuel penetration height, respectively (estimations from the response surface model are used with prediction errors of 0.06%, 0.02% and 0.21%). It indicates that the absolute mixing quantity and fuel penetration are dominantly influenced by the injector length, with a minor effect of the injector location on the former parameter. The total pressure loss primarily depends on the injector length, secondarily affected by the injector location, in agreement with the observations made in Section III.B.

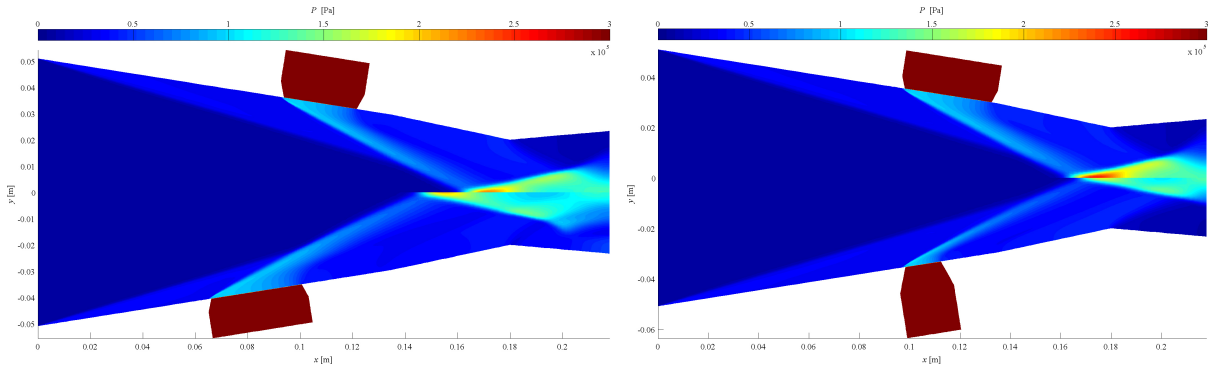

(a) baseline vs S_1 (b) S_2 vs S_3

Figure 9. Comparison of static pressure distributions

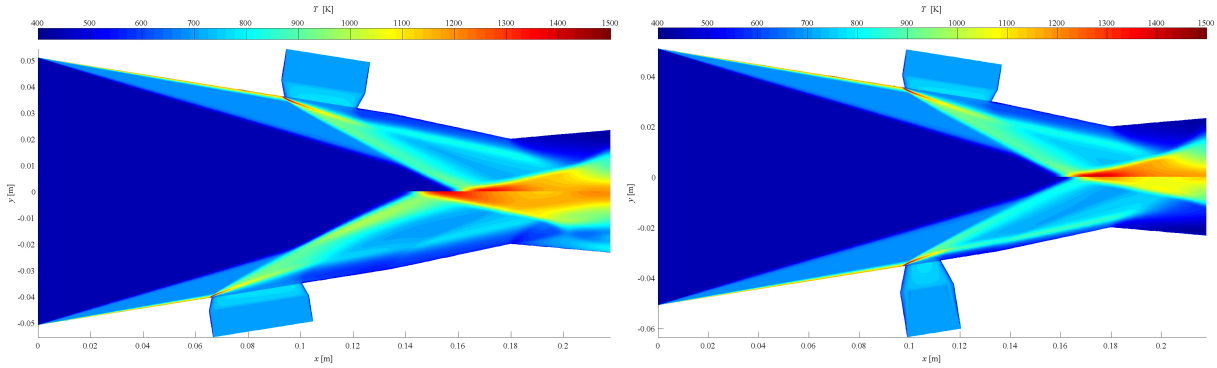

(a) baseline vs S_1 (b) S_2 vs S_3

Figure 10. Comparison of static temperature distributions

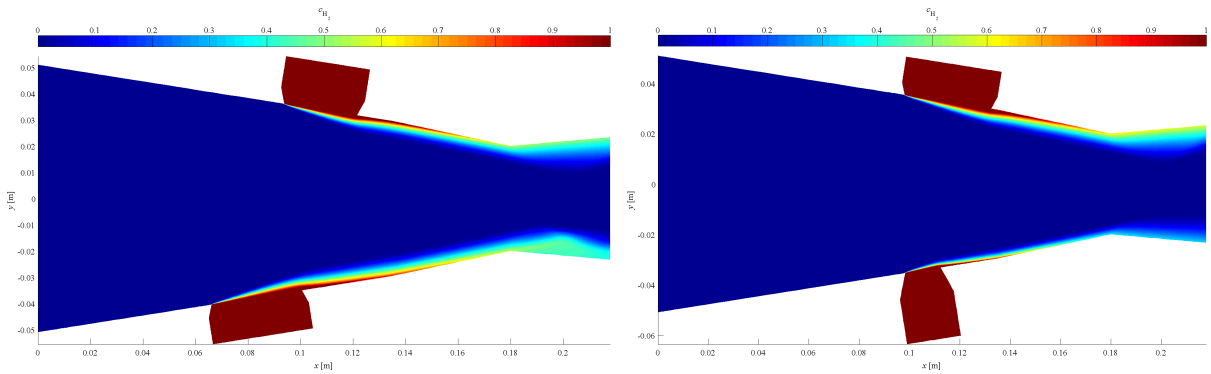

(a) baseline vs S_1 (b) S_2 vs S_3

Figure 11. Comparison of fuel mass fraction distributions

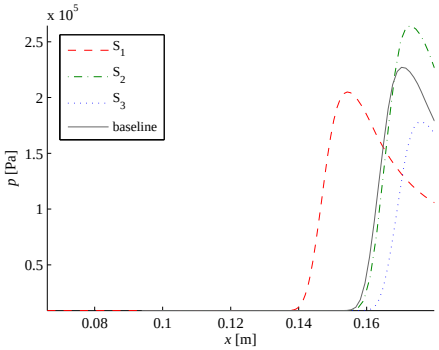

(a) static pressure on symmetry plane

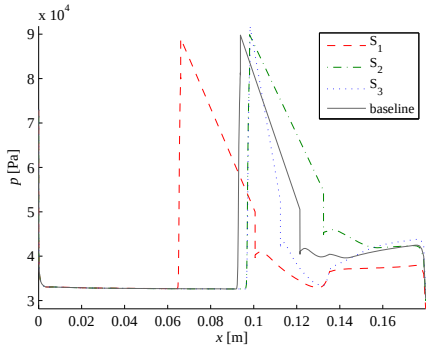

(b) static pressure on inlet wall

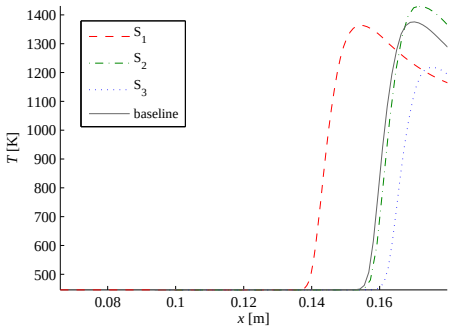

(c) static temperature on symmetry plane

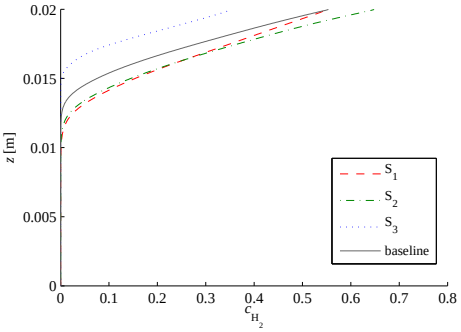

(d) fuel mass fraction at inlet exit

Figure 12. Comparison of various flow property distributions

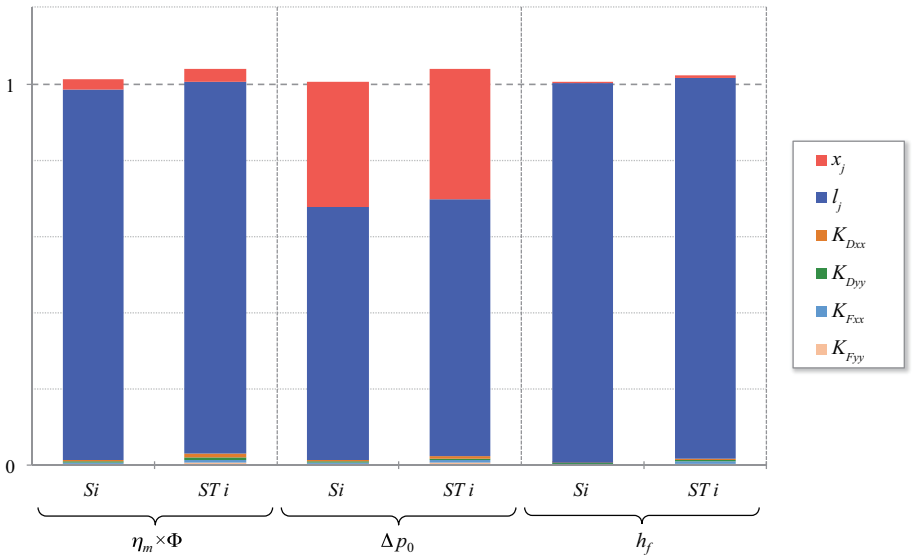

Figure 13. Sensitivity indices for influence of decision variables on objective functions

IV. Conclusions

The present research project is undertaken to investigate the effects of porous properties and geometric variations on the performance of upstream fuel injection via porous media in a scramjet intake, aiming at the application to a class of scramjet engines featuring upstream fuel injection and radical farming concepts.. Two geometric parameters and four porous coefficients are employed as the decision variables for an optimization problem aiming to fulfill three objectives simultaneously, namely, maximum absolute mixing quantity, minimum total pressure loss, and maximum fuel penetration height. The Pareto optimal fronts that resulted from the multi-objective design optimization based on evolutionary algorithms have revealed pronounced counteracting tendencies between the total pressure saving and mixing efficiency as well as the fuel penetration, while the latter two parameters are closely correlated. In particular, the porous injector location and length have been identified as the key design factors that predominantly influence the performance in the aspects considered in the present study, while the porous property has played a negligible role as far as the present configurations and variable ranges are concerned. The analysis of the flowfields has revealed the underlying flow physics, where the structure and intensity of the injection and reflected shock waves are strongly affected by the injector position and size.

Acknowledgment

The authors are grateful to the MDO Group led by Professor Tapabrata Ray at University of New South Wales Canberra for the development of the MDO capability, on which the present extended MDO framework is based. We are thankful to Mr. Markus Kuhn from DLR Stuttgart for information supplied about the physical properties of the porous injectors. We also wish to acknowledge the support of the Australian Research Council (ARC) through the DECRA (Discovery Early Career Researcher Award) Grant No. DE120102277 for Dr. Ogawa.

References

[1]Paull, A., Alesi, H., and Anderson, S., "HyShot Flight Program and How it was Developed", AIAA Paper 2002-5248, Sep 2002.

[2]Boyce, R. R., Gerard, S., and Paull, A., "The HyShot Scramjet Flight Experiment – flight data and CFD calculations compared", AIAA Paper 2003-7029, Dec 2003.

[3]McClinton, C. R., "X-43 – Scramjet Power Breaks the Hypersonic Barrier: Dryden Lectureship in Research for 2006", AIAA Paper 2006-1-317, Jan 2006.

[4]Boeing, "X-51A WaveRider Breaks Record in 1st Flight", `http://boeing.mediaroom.com`, May 2010.

[5]Boyce, R. R., Tirtey, S. C., Brown, L., Creagh, M., and Ogawa, H., "SCRAMSPACE : Scramjet-based Access-to-Space Systems", AIAA Paper 2011-2297, Apr 2011.

[6]Hunt, D. C., Paull, A., Boyce, R. R. and Hagenmaier, M., "Investigation of an axisymmetric scramjet configuration utilising inlet-injection and radical farming", *in Proceedings of the 19th International Symposium on Airbreathing Engines (ISABE 2009)*, Montréal, Sep 2009.

[7]Odam, J. and Paull, A., "Radical Farming in Scramjets", *Notes on Numerical Fluid Mechanics and Multidisciplinary Design*, Vol.96 (*eds.* Tropea,C., Jakirlic,S., Heinemann,H.J., Hinlinger,H.), Springer, Berlin, 2007.

[8]McGuire, J. R., Boyce, R. R., and Mudford, N. R., "Radical farm ignition processes in two-dimensional supersonic combustion", *Journal of Propulsion and Power*, Vol. 24, No. 6, 2008, pp.1248-1257.

[9]Stalker, R. J., Paull, A., Mee, D. J., Morgan, R. G., and Jacobs, P. A., "Scramjets and shock tunnels – The Queensland experience", *Progress in Aerospace Sciences*, Vol. 41, 2005, pp.471-513.

[10]Gruber, M. R., Nejad, A. S., Chen, T. H., and Dutton, J. C., "Bow Shock / Jet Interaction in Compressible Transverse Injection Flowfields", *AIAA Journal*, Vol. 34, No. 10, 1996, pp. pp. 2191-2193.

[11]Wendt, M. N., and Stalker, R. J., "Transverse and parallel injection of hydrogen with supersonic combustion in a shock tunnel", *Shock Waves*, Vol. 6, 1996, pp. 53-59.

[12]Mack, A., Steelant, J., Hannemann, K., Karl, S., and Odam, J., "Mixing and Combustion Enhancement in a Generic Scramjet Combustion Chamber", AIAA Paper 2006-8134, 14$^{\text{th}}$ AIAA/AHI Space Planes and Hypersonic Systems and Technologies Conference, Canberra, Australia, Nov 2006.

[13]Pudsey, A. S., and Boyce, R. R., "Numerical Investigation of Traverse Jets Through Multiport Injector Arrays in Supersonic Crossflow", *Journal of Propulsion and Power*, Vol. 26, No. 6, 2010, pp. 1225-1236.

[14]Schetz, J. A., and Gilreath, H. E., "Tangential Slot Injection in Supersonic Flow",*AIAA Journal*, Vol. 5, No. 12, 1967, pp. 2149-2154.

[15]Billig, F. S., "Research on Supersonic Combustion", *Journal of Propulsion and Power*, Vol. 9, No. 4, 1993, pp. 499-514.

[16]Stalker, R. J., "Control of Hypersonic Turbulent Skin Friction by Boundary-Layer Combustion of Hydrogen", *Journal of Spacecraft and Rockets*, Vol. 42, No. 4, 2005, pp. 577-587.

[17]Sunami, T., Itoh, K., Komuro, T., and Sato, K., "Effects of Streamwise Vortices on Scramjet Combustion at Mach 8-15 Flight Enthalpies – An Experimental Study in HIEST", 17$^{\text{th}}$ International Symposium on Air Breathing Engines, Munich, Germany, Sep 2005.

[18]Kodera, M., Sunami, T., and Itoh, K., "Numerical Simulation of a Scramjet Engine for JAXA 's Flight Experiment Using HyShot," AIAA Paper 2005-3355, 13$^{\text{th}}$ AIAA/CIRA International Space Planes and Hypersonics Systems and Technologies Conference, Naples, Italy, May 2005.

[19]Karagozian, A., Wang, K., Le, A., and Smith, O., "Transverse Gas Jet Injection Behind a Rearward-Facing Step", *Journal of Propulsion and Power*, Vol. 12, No. 6, 1996, pp. 1129-1136.

[20]Takahashi, S., Yamano, G., Wakai, K., Tsue, M., and Kono, M., "Self-Ignition and Transition to Flame-Holding in a Rectangular Scramjet Combustor with a Backward Step", *in Proceedings of the Combustion Institute*, Vol. 28, No. 1, 2000, pp. 705-712.

[21]Schloegel, F., *unpublished data*, The University of Queensland, Australia, 2010.

[22]Capra, B. R., Boyce, R. R., Kuhn, M., and Hald, H., "Porous Versus Porthole Fuel Injection in a Radical Farming Scramjet: A Numerical Analysis", *Journal of Propulsion and Power*, *in print.*

[23]Capra, B., Lorrain, P., Boyce, R. R., Brieschenk, S., Kuhn, M., and Hald, H., "H_2 - O_2 porous fuel injection in a radical farming scramjet", *in Proceedings of the 18th AIAA/3AF International Space Planes and Hypersonic Systems and Technologies Conference*, Tours, France, Sep 2012.

[24]Schloegel, F., Boyce, R. R., McIntyre T. J., and Tirtey, S., "Combustion Scaling in an Inlet Injection Scramjet", AIAA Paper 2012-5811, *in Proceedings of the 18th AIAA/3AF International Space Planes and Hypersonic Systems and Technologies Conference*, Tours, France, Sep 2012.

[25]Ogawa, H, Kodera, M., and Boyce, R. R., "Physical Insight into Hypermixer Injector Design for Fuel/Air Mixing Enhancement in Scramjet Engines via Parametric Numerical Simulations and Surrogate-Assisted Sensitivity Analysis", ISABE-2013-1624, *in Proceedings of the 21st International Symposium on Airbreathing Engines (ISABE 2013)*, Busan, Korea, Sep 2013.

[26]Riggins, D. W. and McClinton, C. R., "Analysis of losses in supersonic mixing and reacting flows", AIAA Paper 91-2266, Jul 1991.

[27]Riggins, D. W., McClinton, C. R., and Vitt, P. H., "Thrust Losses in Hypersonic Engines Part 1: Methodology", *Journal of Propulsion and Power*, Vol. 13, No. 2, 1997, pp. 281-287.

[28]Nield, D. A. and Bejan, A., *Convection in Porous Media*, *Third Edition*, Springer, 2006.

[29]Gascoin, N., Fau, G., Kuhn, P., Gillard, M., Bouchez, M., and Steelant, J., "Comparison of Two Permeation Test Benches and of Two Determination Methods for Darcy 's and Forchheimer's Permeabilities", *Journal of Porous Media*, Vol. 15, No. 8, 2012, pp. 705-720.

[30]Hald, H., Herbertz, A., Kuhn, M., and Ortelt, M., "Technological Aspects of Transpiration Cooled Composite Structures for Thrust Chamber Applications", *in Proceedings of the 16th AIAA/DLR/DGLR International Space Planes and Hypersonic Systems and Technologies Conference*, Bremen, Germany, Oct 2009.

[31]CFD++, *Software Package*, Ver.14.1, Metacomp Technologies Inc., CA, 2014.

[32]Ogawa, H. and Boyce, R. R., "Physical Insight into Scramjet Inlet Behavior via Multi-Objective Design Optimization", *AIAA Journal*, Vol. 50, No. 8, 2012, pp. 1773-1783.

[33]Ogawa, H. and Boyce, R. R., "Nozzle Design Optimization for Axisymmetric Scramjets by Using Surrogate-Assisted Evolutionary Algorithms", *Journal of Propulsion and Power*, Vol. 28, No. 6, 2012, pp. 1324-1338.

[34]Evans, J. S., and Schexnayder, Jr., C. J., "Influence of Chemical Kinetics and Unmixedness on Burning in Supersonic Hydrogen Flames", *AIAA Journal*, Vol. 18, No. 2, 1980, pp. 188-193

[35]Pointwise, *Software Package*, Ver.17.1, Pointwise Inc., TX, 2013.

[36]Deb, K., *Multiobjective Optimization Using Evolutionary Algorithms*, John Wiley & Sons, Ltd., Chichester, UK, 2001.

[37]Deb, K., Pratap, A., Agarwal, S., and Meyarivan, T., "A Fast and Elitist Multiobjective Genetic Algorithm: NSGA-II", *IEEE Transactions on Evolutionary Computation*, Vol. 6, No. 2, 2002, pp. 182-197.

[38]Ogawa, H. and Boyce, R. R., "Multi-Objective Design Optimization of Fuel Injection for Mixing Enhancement in Scramjets by Using Surrogate-Assisted Evolutionary Algorithms", *in Proceedings of the 18th AIAA/3AF International Space Planes and Hypersonic Systems and Technologies Conference*, Tours, France, Sep 2012.

[39]Ray, T., Isaacs, A., and Smith, W., "Multi-Objective Optimization Using Surrogate-Assisted Evolutionary Algorithm", *Multi-Objective Optimization: Techniques and Applications in Chemical Engineering*, World Scientific, Singapore, 2008, pp. 131-151.

[40]Ray, T., and Smith, W., "A Surrogate Assisted Parallel Multiobjective Evolutionary Algorithm for Robust Engineering Design", *Engineering Optimization*, Vol. 38, No. 8, 2006, pp. 997-1011.

[41]Alsumait, J. S., Sykulski, J. K., and Al-Othman, A. K., "A hybrid GA–PS–SQP method to solve power system valve-point economic dispatch problems", *Applied Energy*, Vol. 87, 2010, pp. 1773-1781.

[42]Queipo, N. V., Haftka, R. T., Shyy, W., Goel, T., Vaidyanathan, R., and Tucker, P. K.,"Surrogate-Based Analysis and Optimization", *Progress in Aerospace Sciences*, Vol. 41, 2005, pp. 1-28.

[43]Saltelli, A., Ratto, M., Andres, T., Compolongo, F., Cariboni, J., Gatelli, D., Saisana, M., and Tarantola, S., *Global Sensitivity Analysis. The Primer*, Wiley, Hoboken, NJ, 2008.